Vol. 22 • No. 16 • April 22 • 2010

D10488

www.advmat.de

ADVANCED MATERIALS

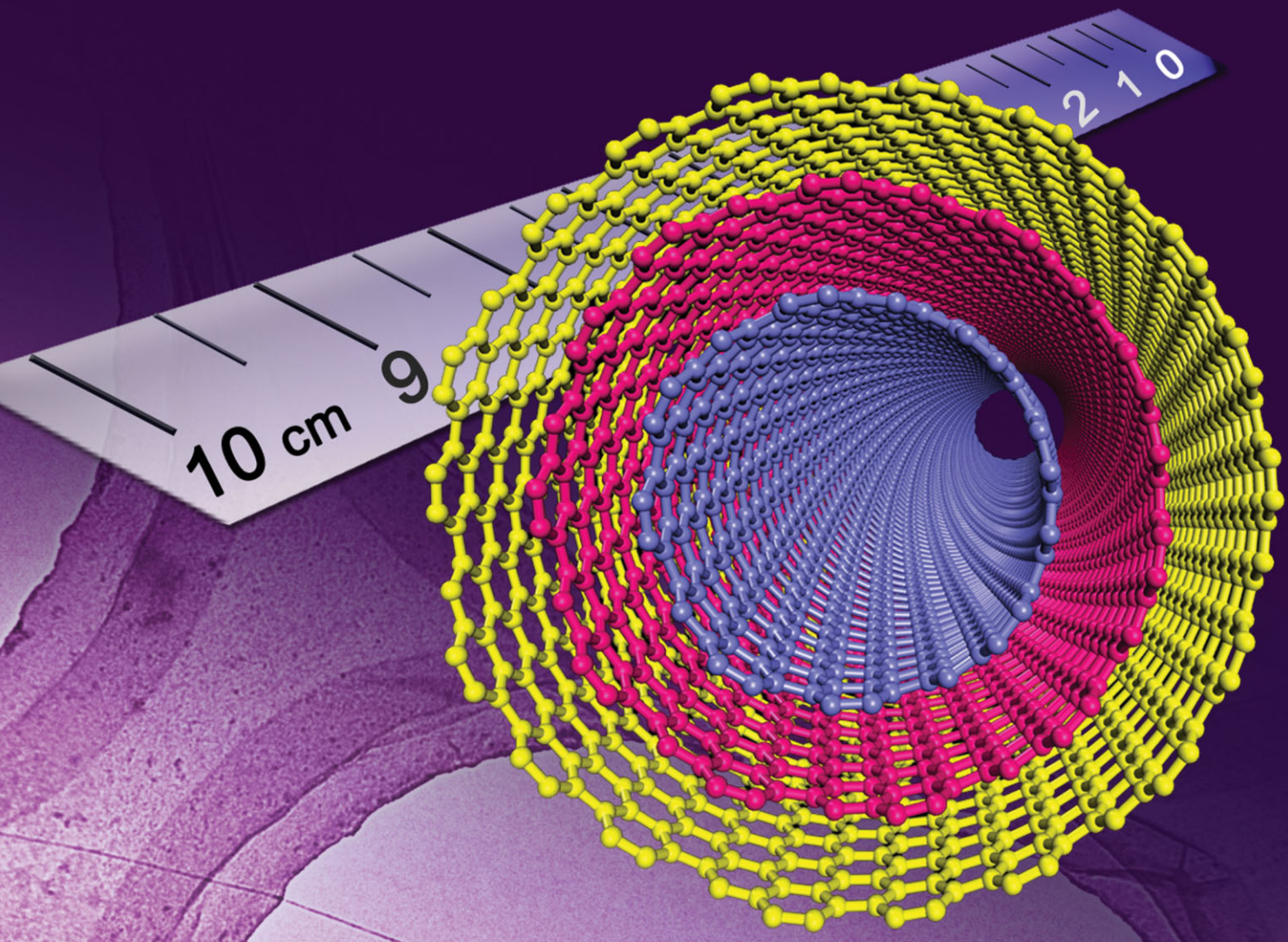

WILEY-VCH

100mm Triple-Walled Carbon Nanotubes

100 mm Long, Semiconducting Triple-Walled Carbon Nanotubes

By *Qian Wen, Weizhong Qian,* Jingqi Nie, Anyuan Cao, Guoqing Ning, Yao Wang, Ling Hu, Qiang Zhang, Jiaqi Huang,* and *Fei Wei**

Carbon nanotubes are considered to be a potential material for next-generation micro- and nanoelectronics, owing to their extraordinary physical properties, such as extremely high mobility ($>10^5\,cm^2\,V^{-1}\,s^{-1}$), ballistic carrier transport, and the ability to carry large current density ($10^9\,A\,cm^{-2}$).[1–5] However, the structural diversity and lack of control of the electronic properties have been major obstacles toward their application in electronics. To this end, a variety of techniques—including the selective growth of semiconducting (versus metallic) nanotubes, electrical breakdown of metallic nanotubes, continued growth, chemical etching and separation of different species—have been extensively investigated.[6–11] By selective growth, a product containing >90% of semiconducting nanotubes can be obtained; however, these nanotubes are still very different in their diameters and bandgaps, and field-effect transistors built on such mixtures have relatively low on/off ratios (<40).[6,7] In addition, selective etching or separation cannot remove the structural difference of the remaining semiconducting nanotubes.[10,11] Despite the progress that has been made, producing a macroscopic material or substrate that contains homogeneous nanotubes remains a major challenge.

Recently, there has been much interest in synthesizing horizontally aligned, ultralong (mm to cm) single-walled nanotubes (SWNTs) or multi-walled tubes (MWNTs).[12–15] In one work, 100 mm long mixed nanotubes were grown by the chemical vapor deposition (CVD) method, but the product contained randomly distributed structures, including SWNTs, double-walled tubes (DWNTs) and MWNTs with many concentric shells,[15] giving rise to the question of structure-controlled growth. When nanotubes are growing, their structure and morphology are susceptible to variations in many environmental factors (e.g., temperature, electrical field, substrate and gas flow),[16–18] and the disturbance of the diameter or helicity often creates intramolecular junctions along the nanotube.[19,20] Though uniform electrical properties were recently demonstrated along a 18.5 cm long SWNT,[21] the uniformity of detailed chiralities along the tube and the mechanism of selective growth still is not fully understood.

Here, we report the direct growth of 100 mm long triple-walled nanotubes (TWNTs) on Si substrates by a gas-flow-directed CVD method. By controlling the narrow window of temperature, gas flow rate, and the concentration of catalyst precursors, a TWNT yield of nearly 90% can be obtained in a controlled way. The smooth transfer of TWNTs from the Si substrate to a transmission electron microscopy (TEM) microgrid allows a clear and exact analysis of the electron diffraction of as-grown TWNTs. The chiral distribution of the tubes suggests a dependent relationship between its length and its metallic or semiconducting shells. Only TWNTs with all three semiconducting shells and narrow distribution of tube chiral angle closing to armchair structure can grow fast (with a rate up to 24 $\mu m\,s^{-1}$) and long (up to 100 mm). Most importantly, we firstly show that long TWNTs possess an unprecedented structural homogeneity in which each shell maintains a constant chiral index extending over a very large distance (>60 mm). In addition, each shell can carry a large current density, in the range of 2×10^8 to $4 \times 10^8\,A\,cm^{-2}$ in a directly fabricated field-effect transistor. Such a semiconducting nanotube material with homogeneous structure along its long length is ideal for specific applications.

Figure 1a and 1b show sparsely distributed individual TWNTs with lengths up to 100 mm that continuously grew from the left edge (where catalyst solution was applied) to the right end of a silicon substrate by CVD at controlled temperature in a period of 60 min. These TWNTs were synthesized by modifying the recently reported CVD methods for growing horizontally aligned, centimeter-long SWNTs.[12–14] Most importantly, we maintained large inter-tube distances (tens to hundreds of micrometers) during growth of the TWNTs (in contrast to other reports),[5,13] and developed a reliable technique to transfer individual TWNTs from the Si substrate onto copper grids for high-resolution TEM (HRTEM) and electron diffraction characterization (see the Supporting Information, Fig. S2). Revealing the atomic structure of as-grown nanotubes allows us to explore the optimized conditions for growing TWNTs with homogeneous structure. A combination of several critical parameters, such as a high gas flow rate (about 100 sccm of CH_4/H_2 mixture with a CH_4/H_2 ratio of 1:5) and catalyst solution concentration (0.03 mol L^{-1} $FeCl_3$ in ethanol), could provide a fast growth (at a rate of about 24 $\mu m\,s^{-1}$)

[*] Prof. W.-Z. Qian, Prof. F. Wei, Q. Wen, J. Q. Nie, Prof. Y. Wang, L. Hu, Dr. Q. Zhang, J. Q. Huang
Beijing Key Laboratory of Green Chemical Reaction Engineering and Technology,
Department of Chemical Engineering, Tsinghua University
Beijing 100084 (PR China)
Fax: +86-10-6277-2051
E-mail: qianwz@mail.tsinghua.edu.cn; wf-dce@tsinghua.edu.cn
Prof. A. Y. Cao
Department of Advanced Materials and Nanotechnology, College of Engineering, Peking University
Beijing 100871 (PR China)
Dr. G. Q. Ning
CNano Technology Limited,
Two Technology St. BDA East District, Beijing 100023 (PR China)

DOI: 10.1002/adma.200902746

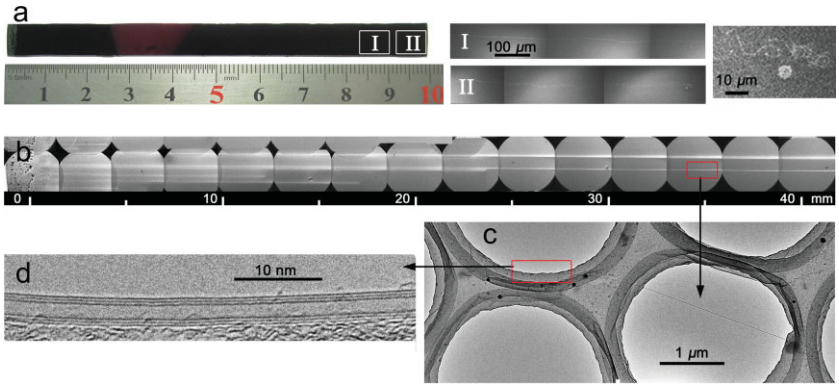

Figure 1. 100 mm long TWNTs. a) (Left) Picture of the 100 mm long Si substrate on which individual TWNTs were grown continuously from the left to the right edge of the substrate; (Middle) Scanning electron microscopy (SEM) images of the end segments of a 100 mm long TWNT; (Right) The end of TWNT with a catalyst particle. b) SEM images of the region where the growth started (0 to 40 mm on the Si substrate) showing horizontally aligned, straight TWNTs. About 24 images (circular background) were put together to cover a length scale of 40 mm. c) TEM image of a portion of the TWNT (enclosed by the red rectangle in b) transferred to TEM grids. d) HRTEM image showing a triple-walled structure of the as-grown tube.

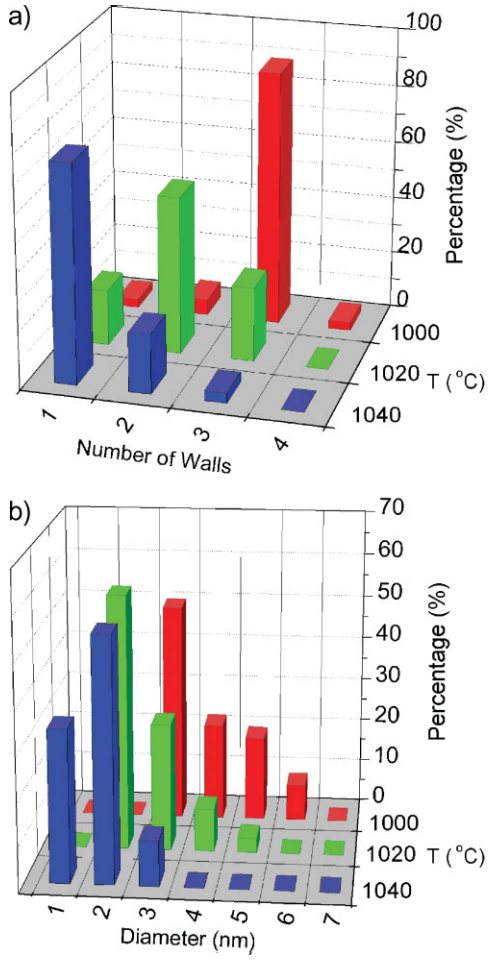

Figure 2. Structure distribution of CNTs grown at different temperatures: a) Distribution of numbers of walls of centimeter long CNTs; and, b) Distribution of outer diameters of centimeter-long CNTs.

of TWNTs with sufficient buoyancy to resist contact to the substrate and avoid early termination of the growth process. The catalyst particle observed at the end of TWNTs suggests a kite-growth mechanism, as has been proposed previously.[13,14] In comparison, the growth rate (about 10 to 20 $\mu m\,s^{-1}$) of SWNTs synthesized by other groups is close to our TWNTs (24 $\mu m\,s^{-1}$).[12–14]

Selected segments of individual TWNTs were transferred to TEM grids assisted by a cellulose acetate film (see the Supporting Information, Fig. S2) for HRTEM examination, which revealed a clean, triple-walled structure with a uniform outer diameter of 3.1 nm (Fig. 1c and d). The aspect-ratio of this 100 mm TWNT was as high as 3×10^7. The process does not show preference for tube type, and all SWNTs, DWNTs and TWNTs can be transferred to TEM grids. Based on TEM, we carefully calculated the diameter and number of walls of 96 CNTs (centimeter-long, on about 50 substrates) grown at different temperatures, as shown in Figure 2. The growth of the triple-walled structure is sensitive to the CVD temperature, and we could control the yield of TWNTs to be nearly 90% at 1000 °C. Small increases of temperature, by 20 and 40 °C, resulted in a high yield of DWNTs (>50%) and SWNTs (>70%), respectively (Fig. 2a). The relative outer diameter of nanotubes increased from <3 nm to a distribution of 2–6 nm (Fig. 2b). Although many techniques have been developed to synthesize high-purity SWNT films, DWNT buckypapers and MWNTs with larger shell numbers, the exclusive growth of pure and long TWNTs has not been reported previously.

We characterized the long-range structural homogeneity of these 100 mm long TWNTs by recording HRTEM images and electron diffraction patterns at many positions with large distances along the tube length (e.g., 25, 27, 32, 45, 47, 60 and 70 mm) (Fig. 3 and Fig. S6 in the Supporting Information). The chiral indices, (n, m), of all the three shells at any cross section in the TWNT could be determined accurately (see the Supportin Information, Fig. S7–S9).[22,23] The results show that this TWNT maintains a constant chiral index for each shell through the length of 25 to 60 mm (electron diffraction patterns of these two positions were shown in Fig. 3b), which were assigned to (13, 8), (21, 11) and (25, 18), from the inner to outer shell, respectively. The diameter and chiral angle of the inner, middle and outer shell before the length of 60 mm were 1.44 nm and 22.2°, 2.21 nm and 19.8°, 2.93 nm and 24.6°, respectively. The inter-shell distances were 0.384 nm (between the inner and middle shell) and 0.36 nm (between the middle and outer shell), while in a quadruple-walled nanotube the inter-shell distance was found to vary from 0.36 to 0.5 nm.[22] Although the three shells in this TWNT have different helicities, they are all semiconducting according to their chiral indices in which $n - m \neq 3k$ (where k is a non-zero integer). Since TWNTs were grown at a very low density (except close to the catalyst-loaded region), the absence of interactions between adjacent tubes, such as bundling or entangling, is also favorable

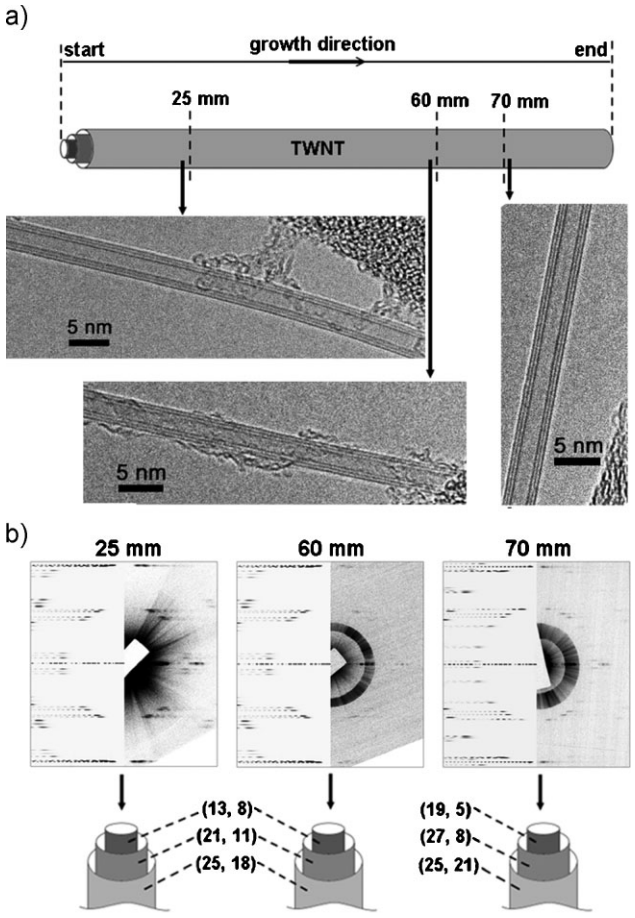

Figure 3. Long-range homogeneous atomic-structure of TWNTs. a) Illustration of a 100 mm long TWNT and HRTEM images on three positions that are 25, 60 and 70 mm away from the growth-starting point. b) Electron diffraction patterns recorded on the TWNT at these three positions, and the chiral indices assigned to all three shells at each location.

for maintaining a straight morphology and undisturbed structure during growth. Our results demonstrate a continuous growth of TWNTs at a high speed without change of the diameter and helicity in any of the three shells, therefore keeping a homogeneous structure for a length of up to 60 mm.

The chiral indices of the inner to outer shells at the length of 70 mm were assigned as (19, 5), (27, 8) and (25, 21), respectively, corresponding to diameters and chiral angles of 1.71 nm and 11.4° (inner shell), 2.49 nm and 12.6° (middle shell), 3.12 nm and 27.1° (outer shell), respectively. There was an increase of tube diameter across this region (60 to 70 mm), by different degrees for each shell (7–20%). The change of chiral angles seems random, with the inner and middle shell showing a considerable drop from about 20° to 12°. The structural change occurred after a length of 70 mm along the TWNT is likely due to the temperature change near the end of the constant-temperature zone in our CVD system. Despite such diameter and helicity changes, all the shells remain semiconducting through the entire length of the TWNT.

In order to understand the growth mechanism of such endless TWNTs, we characterized eight TWNTs with different

Table 1. Chiral indices, diameters and chiral angles of eight TWNTs with different lengths.

Number	Length [mm]	Diameter [nm]	(*n*, *m*)	Chiral angle α [deg]	$\Delta\alpha$ [deg]	Semiconducting or metallic
1	60	1.36	11, 9	26.7	4.1	s
		2.12	19, 12	22.6	0.4	s
		2.87	26, 16	22.2		s
2	40	2.71	21, 19	28.3	2.7	s
		3.60	30, 23	25.6	3.3	s
		4.34	33, 31	29.0		s
3	30	1.44	13, 8	22.2	2.4	s
		2.21	21, 11	19.8	4.9	s
		2.93	25, 18	24.6		s
4	10	3.43	32, 18	20.8	3.4	s
		4.31	43, 19	17.4	1.1	m
		5.12	50, 24	18.5		s
5	7	3.56	30, 20	23.4	6.3	s
		4.38	44, 19	17.1	2.6	s
		5.03	48, 25	19.7		s
6	6	1.64	18, 5	11.9	2.0	s
		2.26	24, 8	13.9	3.8	s
		3.10	35, 8	10.1		m
7	2	3.78	35, 20	21.1	4.3	m
		4.46	45, 19	16.8	1.5	s
		5.19	51, 24	18.3		m
8	2	1.72	19, 5	11.4	1.9	s
		2.46	28, 6	9.5	5.0	s
		3.23	34, 12	14.6		s

lengths. We found that all tubes longer than 30 mm contained only semiconducting shells, while several shorter tubes (<10 mm) had one or two metallic shells (Table 1). That is probably because the electric field induced from the heating coil of the tube reactor can influence and disrupt the smoothly flying of metallic tubes via a kite-mechanism, leading to early termination of their growth, since the static polarizability of metallic nanotubes is nearly three orders of magnitude larger than that of semiconducting nanotubes.[24] Under the same condition, TWNTs without metallic shells are less influenced and could keep a steady floating until a much longer time (and tube length). Our results indicate a length-dependent selective growth of long TWNTs with exclusively semiconducting shells, as illustrated in Figure 4a. Selective growth of semiconducting TWNTs is significant given that tubes with multiple shells are very likely to contain metallic shells, for example, DWNTs and MWNTs were frequently observed to consist of both semiconducting and metallic shells mixed in the same tube.[8,25] Calculations showed that semiconducting tubes (shells) have lower energies resulting in their preferential formation versus metallic shells.[26] In addition, shells longer than 30 mm have relatively larger chiral angles (20°–30°) than most of shorter shells (10°–20°) (Fig. 4b). Larger chiral angles were also observed in double-walled nanotubes.[27] The difference between the chiral angles of the shells in the same TWNT is small ($\Delta\alpha < 6.3°$). Our results suggest that the TWNT consisting of semiconducting shells with larger chiral angles is a relatively stable structure that is amenable to high-rate and long-range growth. The wide

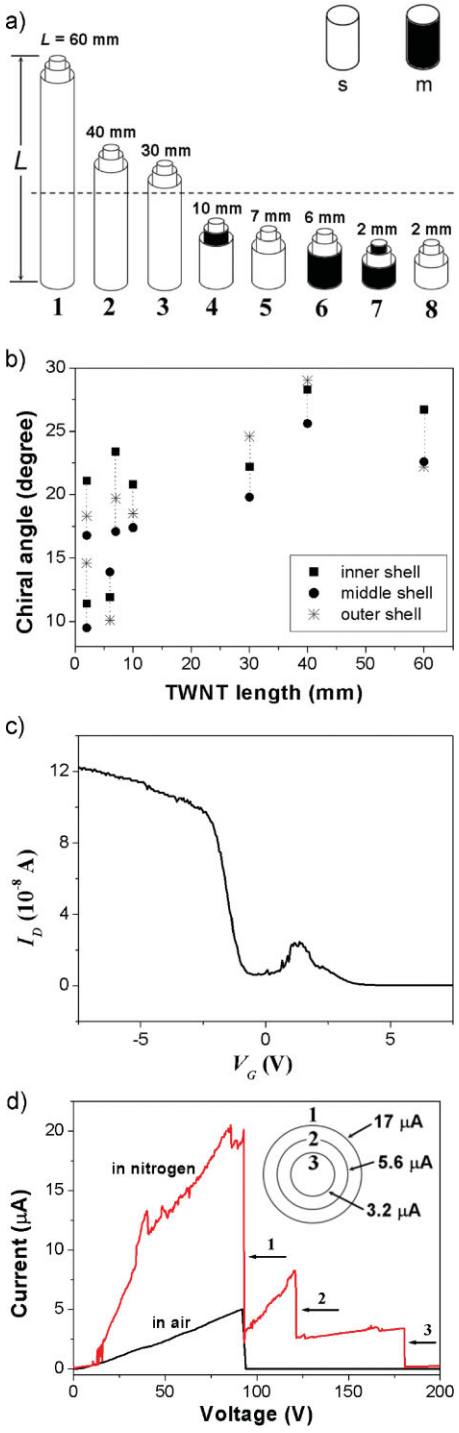

Figure 4. Length-dependent growth of semiconducting TWNTs and electronic properties. a) Illustration of eight TWNTs (listed in Table 1) showing the selective growth of long (>30 mm), semiconducting TWNTs; "s" and "m" indicate semiconducting and metallic shells, respectively. b) The chiral angle distribution of TWNTs with different lengths. c) Current versus gate voltage (V_G) characteristics at a constant bias of 1 V of a typical FET device with an on/off ratio of 4800 fabricated on the semiconducting TWNT in Figure 2a. d) Current flow through individual TWNTs measured in air and nitrogen. The arrows (labeled 1, 2, and 3) indicate shell breakdowns occurred during the failure. Inset, illustration of the current-carrying capability of each shell in the TWNT.

range of chiral indices observed in Table 1 indicates great structural diversity among TWNTs and their shells, even when they were grown under the same CVD conditions. However, those long TWNTs all possess a high-degree of structural homogeneity with constant chiral indices of three shells throughout their lengths.

The semiconducting TWNT shown in Figure 3 can be fabricated into FETs with p-type characteristics (Fig. 4c). Preliminary tests on FETs at different positions of this TWNT show consistent device performance with on/off ratios (I_{on}/I_{off}) in the range of 3000 to 5000. Devices built on TWNTs containing metallic shells cannot be turned off. In addition, a single TWNT (device length of 0.5 to 1 mm) can carry a current of 5 μA at room temperature in air, and about 20 μA in nitrogen (Fig. 4d). The current-carrying capability of TWNTs is comparable to high-quality SWNTs with Pd contacts in vacuum (approximately 25 μA per tube) and multi-walled tubes made by the arc technique (approximately 19 μA per shell).[4,9] The three shells of this TWNT simultaneously carry the current flow, and breakdowns of individual shells were clearly observed in nitrogen, where the current dropped by 17, 5.6, and 3.2 μA, respectively (Fig. 4d). Based on the breakdown sequence, as observed in larger-diameter (9.5 nm) multi-walled tubes previously,[9] we suppose the breakdown of this TWNT is from the outer (diameter = 2.6 nm), to the middle (1.82 nm) and then to the inner shell (1.05 nm), and the maximum current density sustained by each shell (from outer to inner) is 3.2×10^8, 2.15×10^8, and 3.7×10^8 A cm^{-2}, respectively. In comparison, the highest current density measured in short, ballistic SWNTs is on the order of 10^9 A cm^{-2}.[4] The FET performance and current density could be further improved by using better electrical contacts (e.g., Pd) and testing in high vacuum. Compared with SWNTs, TWNTs could offer several additional advantages such as less bundling, enhanced and tunable mechanical strength (e.g., by inter-shell crosslinking), and sustaining larger currents (by all the shells).

In summary, we demonstrate the gas flow-directed growth method used here is effective to obtain semiconducting TWNTs of uniform structure and as long as 100 mm. The chiral angle distributions of the centimeter long TWNTs are apparently between 20° and 30°, indicating the extremely high growth rate of 24 μm s^{-1} results in a high selectivity of CNTs with definite structure. This method also implies an effective method to selectively grow semiconducting MWNTs. Concentric shells with controlled electronic properties also bring the opportunity to construct co-axial devices. The long range homogenous TWNT structure could be a platform to make high-density, reproducible nanodevices as well as integrated logic circuits that can be assembled on a single nanotube.[28]

Experimental

Substrates: The substrate we used here was a 4 inch Si wafer (p-type, 111, ~10 Ω cm, 500 μm in thickness) purchased from Grinm Semiconductor Materials Co., Ltd., Beijing. 700 nm SiO_2 was thermal oxidized on the surface. The substrate was cut into rectangle sheets about 10 cm long and 1 cm wide. They were ultrasonicated and washed in acetone, ethanol, de-ionized water for 5 min in sequence. Then the

substrate was dried in air at 200 °C ready for catalyst spreading and CNT growth.

Catalyst: The reagents ($FeCl_3 \cdot 6H_2O$ and ethanol) were provided by Beijing Yili chemical company. Ethanol solution of $FeCl_3$ (0.03 mol L^{-1}) was dropped onto one edge of Si substrate to form a catalyst source region with only 1 mm width from the edge of the substrate. The ethanol solution quickly vaporized as soon as it was spread and then it was ready for the growth of CNTs.

Synthesis Process: The Si wafer carrying the catalyst was placed into the center of a 1.0 m long quartz tube (30 mm in diameter) furnace. The temperature distribution of the furnace is shown in Figure S1 in the Supporting Information. The catalyst source region was placed near the gas entrance and the long Si sheet was directed toward the gas flow. The substrate was heated at 900 °C for 10 min in a hydrogen atmosphere. When the temperature was increased to 1000 °C, the mixture of CH_4 and H_2 (about 100 sccm with CH_4/H_2 ratio of 1:5) was fed into the reactor for 100 min. Then the growth was stopped by switching off the reactant gas and the furnace was cooled in argon to room temperature.

Characterization: The CNTs were characterized by scanning electron microscopy (SEM, JSM7401F, 1 kV), high-resolution transmission electron microscopy (HR-TEM, JEM-2010, 120 kV), and a semiconductor parameter characterization system (Agilent 4156C). In order to detailed characterize the TWNTs by TEM to understand their structure, cellulose acetate film (60 μm in thickness) purchased from Beijing XXBR Technology Co., Ltd. was used to transfer the super-long CNTs from the Si substrate to the TEM grid. The detailed transfer procedure is described in Figure S2 in the Supporting Information.

Acknowledgements

This work was supported by NSFC (20606020), FANEDD (200548), and the China National Program (2006CB932702). We are grateful to Prof. Yan Li and Mr. Yagang Yao, Prof. Kaili Jiang and Prof. Qunqing Li, Dr. Hua Jiang, and Prof. Dangsheng Su for help in the experiment details, the I–V characterizations, the analysis of electron diffractions by TEM and discussions about the results, respectively. Supporting Information is available online from Wiley InterScience or from the author.

Received: August 11, 2009
Revised: October 13, 2009
Published online: January 7, 2010

[1] A. Jorio, G. Dresselhaus, M. S. Dresselhaus, *Carbon Nanotubes: Advanced Topics in the Synthesis, Structure, Properties and Applications*, Springer-Verlag, Berlin Heidelberg, **2008**.
[2] R. H. Baughman, A. A. Zakhidov, W. A. de Heer, *Science* **2002**, *297*, 787.
[3] A. P. Graham, G. S. Duesberg, R. V. Seidel, M. Liebau, E. Unger, W. Pamler, F. Kreupl, W. Hoenlein, *Small* **2005**, *1*, 382.
[4] A. Javey, J. Guo, Q. Wang, M. Lundstrom, H. J. Dai, *Nature* **2003**, *424*, 654.
[5] S. J. Kang, C. Kocabas, T. Ozel, M. Shim, N. Pimparkar, M. A. Alam, S. V. Rotkin, J. A. Rogers, *Nat. Nanotechnol.* **2007**, *2*, 230.
[6] Y. M. Li, D. Mann, M. Rolandi, W. Kim, A. Ural, S. Hung, A. Javey, J. Cao, D. W. Wang, E. Yenilmez, Q. Wang, J. F. Gibbons, Y. Nishi, H. J. Dai, *Nano Lett.* **2004**, *4*, 317.
[7] L. Ding, A. Tselev, J. Y. Wang, D. N. Yuan, H. B. Chu, T. P. McNicholas, Y. Li, J. Liu, *Nano Lett.* **2009**, *9*, 800.
[8] Y. H. Wang, M. J. Kim, H. W. Shan, C. Kittrell, H. Fan, L. M. Ericson, W. F. Hwang, S. Arepalli, R. H. Hauge, R. E. Smalley, *Nano Lett.* **2005**, *5*, 997.
[9] P. G. Collins, M. S. Arnold, P. Avouris, *Science* **2001**, *292*, 706.
[10] G. Y. Zhang, P. F. Qi, X. R. Wang, Y. R. Lu, X. L. Li, R. Tu, S. Bangsaruntip, D. Mann, L. Zhang, H. J. Dai, *Science* **2006**, *314*, 974.
[11] M. S. Arnold, A. A. Green, J. F. Hulvat, S. I. Stupp, M. C. Hersam, *Nat. Nanotechnol.* **2006**, *1*, 60.
[12] L. X. Zheng, M. J. O'Connell, S. K. Doorn, X. Z. Liao, Y. H. Zhao, E. A. Akhadov, M. A. Hoffbauer, B. J. Roop, Q. X. Jia, R. C. Dye, D. E. Peterson, S. M. Huang, J. Liu, Y. T. Zhu, *Nat. Mater.* **2004**, *3*, 673.
[13] Z. Jin, H. B. Chu, J. Y. Wang, J. X. Hong, W. C. Tan, Y. Li, *Nano Lett.* **2007**, *7*, 2073.
[14] S. M. Huang, M. Woodson, R. Smalley, J. Liu, *Nano Lett.* **2004**, *4*, 1025.
[15] B. H. Hong, J. Y. Lee, T. Beetz, Y. M. Zhu, P. Kim, K. S. Kim, *J. Am. Chem. Soc.* **2005**, *127*, 15336.
[16] Y. G. Yao, Q. W. Li, J. Zhang, R. Liu, L. Y. Jiao, Y. T. Zhu, Z. F. Liu, *Nat. Mater.* **2007**, *6*, 283.
[17] G. W. Ho, A. T. S. Wee, J. Lin, *Appl. Phys. Lett.* **2001**, *79*, 260.
[18] N. Geblinger, A. Ismach, E. Joselevich, *Nat. Nanotechnol.* **2008**, *3*, 195.
[19] M. Ouyang, J. L. Huang, C. L. Cheung, C. M. Lieber, *Science* **2001**, *291*, 97.
[20] Z. Yao, H. W. C. Postma, L. Balents, C. Dekker, *Nature* **1999**, *402*, 273.
[21] X. S. Wang, Q. Q. Li, J. Xie, Z. Jin, J. Y. Wang, Y. Li, K. L. Jiang, S. S. Fan, *Nano Lett.* **2009**, *9*, 3137.
[22] Z. J. Liu, Q. Zhang, L. C. Qin, *Appl. Phys. Lett.* **2005**, *86*, 191903.
[23] H. Jiang, D. P. Brown, P. Nikolaev, A. G. Nasibulin, E. I. Kauppinen, *Appl. Phys. Lett.* **2008**, *93*, 141903.
[24] E. Joselevich, C. M. Lieber, *Nano Lett.* **2002**, *2*, 1137.
[25] M. Gao, J. M. Zuo, R. Zhang, L. A. Nagahara, *J. Mater. Sci.* **2006**, *41*, 4382.
[26] Y. M. Li, S. Peng, D. Mann, J. Cao, R. Tu, K. J. Cho, H. J. Dai, *J. Phys. Chem. B* **2005**, *109*, 6968.
[27] K. Hirahara, M. Kociak, S. Bandow, T. Nakahira, K. Itoh, Y. Saito, S. Iijima, *Phys. Rev. B* **2006**, *73*, 195420.
[28] Z. H. Chen, J. Appenzeller, Y. M. Lin, J. Sippel-Oakley, A. G. Rinzler, J. Y. Tang, S. J. Wind, P. M. Solomon, P. Avouris, *Science* **2006**, *311*, 1735.